Effects of Microsolvation on the Adenine−Uracil Base Pair and Its Radical Anion: Adenine−Uracil Mono- and Dihydrates†

Sunghwan Kim and Henry F. Schaefer, III*

Center for Computational Chemistry, University of Georgia, Athens, Georgia 30602

Received: April 6, 2007; In Final Form: May 25, 2007

Microhydration effects upon the adenine−uracil (AU) base pair and its radical anion have been investigated by explicitly considering various structures of their mono- and dihydrates at the B3LYP/DZP++ level of theory. For the neutral AU base pair, 5 structures were found for the monohydrate and 14 structures for the dihydrate. In the lowest-energy structures of the neutral mono- and dihydrates, one and two water molecules bind to the AU base pair through a cyclic hydrogen bond via the N_9-H and N_3 atoms of the adenine moiety, while the lowest-lying anionic mono- and dihydrates have a water molecule which is involved in noncyclic hydrogen bonding via the O_4 atom of the uracil unit. Both the vertical detachment energy (VDE) and adiabatic electron affinity (AEA) of the AU base pair are predicted to increase upon hydration. While the VDE and AEA of the unhydrated AU pair are 0.96 and 0.40 eV, respectively, the corresponding predictions for the lowest-lying anionic dihydrates are 1.36 and 0.75 eV, respectively. Because uracil has a greater electron affinity than adenine, an excess electron attached to the AU base pair occupies the π^* orbital of the uracil moiety. When the uracil moiety participates in hydrogen bonding as a hydrogen bond acceptor (e.g., the $N_6-H_{6a}\cdots O_4$ hydrogen bond between the adenine and uracil bases and the $O_w-H_w\cdots N$ and $O_w-H_w\cdots O$ hydrogen bonds between the AU pair and the water molecules), the transfer of the negative charge density from the uracil moiety to either the adenine or water molecules efficiently stabilizes the system. In addition, anionic structures which have $C-H\cdots O_w$ contacts are energetically more favorable than those with $N-H\cdots O_w$ hydrogen bonds, because the $C-H\cdots O_w$ contacts do not allow the unfavorable electron density donation from the water to the uracil moiety. This delocalization effect makes the energetic ordering for the anionic hydrates very different from that for the corresponding neutrals.

Introduction

Carcinogenic and mutagenic effects[1−8] of high-energy radiation arise from the ability of photons to produce lethal DNA lesions such as modified bases,[9−11] abasic sites,[12−15] interstrand cross-links,[16−19] and single- and double-strand breaks (SSBs and DSBs).[20−22] At an initial step of radiation-induced DNA damage, radiation generates positive holes within the DNA duplex by ionizing the nucleic acid bases (NABs).[23−30] Migration of these positive charges tends toward guanine sites, leading to formation of various oxidative products.[31−37] On the other hand, ionizing radiation can cause DNA damage not only through the direct hit by high-energy quanta, but also through the interaction of DNA components with low-energy electrons (LEEs),[38−44] which are mainly generated by radiolysis of water.[45] Moreover, many experimental and theoretical studies proved that LEEs even at energies of zero or near-zero eV can induce DNA damage.[46−52]

Recently, Sanche and co-workers[53] qualitatively analyzed various radiation products that were generated by irradiating solid thin films of tetrameric nucleotides with 10 eV electrons under ultrahigh vacuum. On the basis of the distribution of the radiation products, Sanche suggested that an initial step in DNA damage by LEEs involves electron attachment to the NABs, followed by electron transfer to the sugar−phosphate backbone and subsequent dissociation of the phosphodiester bond. Similarly, in recent theoretical studies using density functional theory (DFT), Leszczynski and co-workers[49,50] demonstrated that the attachment of LEEs to NABs can give rise to DNA strand breaks by C3′−O3′ or C5′−O5′ σ-bond cleavage. In this respect, the electron affinities of the NABs are of importance in understanding the mechanism of radiation-induced DNA damage.

While most of early ab initio studies predicted negative adiabatic electron affinities for all NABs, Adamowicz and co-workers[54−56] suggested the existence of the dipole bound anions in which an electron is trapped in a dipole field of the neutral molecule. Desfrancois et al.[57] employed Rydberg electron transfer (RET) spectroscopy to detect the dipole-bound anions of uracil, thymine, and adenine. The adiabatic electron affinities (AEAs) arising from these dipole-bound anionic states were determined to be 0.054 ± 0.035, 0.068 ± 0.020, and 0.012 ± 0.005 eV for uracil, thymine, and adenine, respectively. Using negative ion photoelectron spectroscopy, Bowen and co-workers[58] also detected the dipole-bound anions of uracil and thymine. However, the existence of the dipole bound states in aqueous phases seems improbable, because the former are strongly destabilized in condensed or aqueous phases due to their diffuse character.[59] Instead, the valence-bound anions are thought to be the predominant form of NAB negative ions in aqueous solution and in living organisms.

While the gas-phase AEAs of the NABs arising from the valence anionic states are thought to be negative or near zero eV,[60] hydration effects in aqueous solution are known to increase the AEAs of NABs.[61−64] Using photodetachment−photoelectron spectroscopy, Schiedt, Weinkauf, Neumark, and Schlag[61] found

† Part of the special issue "Robert E. Wyatt Festschrift".

* Corresponding author. E-mail: hfs@uga.edu.

10.1021/jp072727g CCC: $37.00
Published on Web 08/18/2007

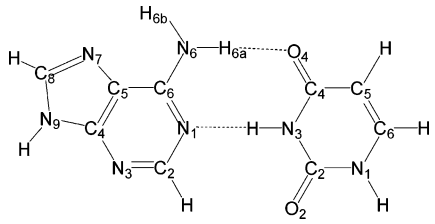

Figure 1. Atom numbering scheme for the Watson−Crick adenine−uracil base pair.

that the AEAs of three pyrimidine NABs, uracil, thymine, and cytosine linearly increase with the number of hydrating molecules. While the gas-phase AEAs of the isolated NABs, estimated in that study by extrapolating from the water clusters of the NABs, were 0.15, 0.12, and 0.13 eV for uracil, thymine, and cytosine, respectively, the AEAs for the analogous pentahydrates increased up to 1.0 eV for all three bases. Thus, investigation of hydration effects upon the AEAs of the NABs is essential to understanding the mechanism of radiation-induced DNA damage.

Although the water complexes of the isolated DNA/RNA bases have been studied extensively both experimentally[65−69] and theoretically,[62−64,70−75] there have been relatively few studies reported on hydration effects for the base pairs.[76−78] In the present research, we have studied microhydration effects on the electron affinity of the adenine−uracil (AU) base pair by explicitly considering various structures of mono- and dihydrates of the AU base pair and its anion.

Theoretical Methods

The Q-Chem 3.0 package of programs[79] has been used for all geometry optimizations and vibrational frequency analyses. Neutral mono- and dihydrates of the Watson−Crick AU base pair (Figure 1) have been optimized using the B3LYP density functional, which is Becke's three-parameter exchange functional (B3),[80] in conjunction with the correlation functional of Lee, Yang, and Parr (LYP).[81] For numerical integrations, an Euler-Maclaurin-Lebedev-(75,302) grid, having 75 radial shells and 302 angular points per shell, was employed.[82] We used double-ζ quality basis sets with polarization and diffuse functions (DZP++).[83−86] Theoretical details may be found in refs 62−64. This amounts to 427 and 458 contracted Gaussian basis functions for the mono- and dihydrates of the AU base pair, respectively.

The geometries of the anionic hydrates of the AU base pair were optimized at the same level of theory, using the optimized geometries of the corresponding neutrals as initial geometries. The vertical detachment energy (VDE) for each anionic structure was evaluated according to the following definition:

$$\mathrm{VDE} = E(\text{neutral at optimized anion geometry}) - E(\text{optimized anion})$$

Because there were multiple local minima for both the AU hydrates and their anions, we considered two types of the AEA: the local AEA ($\mathrm{AEA_{local}}$) and the absolute AEA ($\mathrm{AEA_{abs}}$), which are given as the following equations:

$$\mathrm{AEA_{local}} = E(\text{optimized neutral}) - E(\text{optimized anion})$$

$$\mathrm{AEA_{abs}} = E(\text{global minimum optimized neutral}) - E(\text{global minimum optimized anion})$$

The $\mathrm{AEA_{local}}$ is the energy difference between a local minimum of a neutral hydrate and the corresponding anionic local minimum, found from geometry optimization using the geometry of that neutral hydrate as an initial geometry. On the other hand, the $\mathrm{AEA_{abs}}$ is the energy difference between the global minimum on the potential surfaces of the neutral species and that of the anionic species. In the present study, the AEA refers to the $\mathrm{AEA_{local}}$ unless explicitly specified as $\mathrm{AEA_{abs}}$.

We assumed that all water molecules are approximately located in the molecular plane of the AU base pair because all hydrogen bond donors (N−H hydrogen atoms) and acceptors (σ-type lone pairs on N and O atoms) of the AU base pair are in the molecular plane. Of course, this assumption may preclude some structures where water molecules are above or below the molecular plane. In recent theoretical studies on anionic and neutral hydrates of uracil,[74,75] water molecules in all structures for the mono- and dihydrates were predicted to be roughly in the molecular plane of uracil,[74] while binding of out-of-plane water molecules appeared in higher hydrates.[75] Therefore, our assumption employed in the present study seems appropriate for the mono- and dihydrates of the AU base pair.

TABLE 1: Relative Energies (E_{rel}) and Hydration Energies (E_{hyd}) in kcal mol^{-1} of Mono- and Dihydrates of the AU Base Pair and Their Respective Anions (ZPVE-corrected Values in Parentheses) (See Texts for Notation Concerning the Different Structures)

structure	E_{rel}[a]		E_{hyd}[b]		structure	E_{rel}[a]		E_{hyd}[c]	
1A	0.0	(0.0)	11.2	(8.9)	**1A**$^-$	0.6	(0.6)	12.9	(10.8)
1B	0.3	(0.3)	10.8	(8.5)	**1B**$^-$	0.7	(0.8)	12.8	(10.6)
1C	1.1	(1.4)	10.1	(7.5)	**1C**$^-$	4.1	(3.4)	9.5	(8.0)
1D	4.2	(3.8)	6.9	(5.1)	**1D**$^-$	0.0	(0.0)	13.5	(11.4)
1E	5.9	(5.3)	5.2	(3.6)	**1E**$^-$	2.0	(2.1)	11.5	(9.3)
2A	0.0	(0.0)	24.0	(19.2)	**2A**$^-$	0.2	(0.4)	26.1	(21.6)
2B	0.5	(0.6)	23.5	(18.6)	**2B**$^-$	2.1	(2.2)	24.2	(19.8)
2C	2.1	(1.9)	21.9	(17.4)	**2C**$^-$	0.7	(0.7)	25.7	(21.3)
2D	2.3	(2.4)	21.7	(16.8)	**2D**$^-$	3.5	(2.8)	22.8	(19.1)
2E	3.0	(3.1)	21.0	(16.1)	**2E**$^-$	4.2	(3.6)	22.2	(18.3)
2F	5.9	(5.3)	18.1	(14.0)	**2F**$^-$	0.0	(0.0)	26.3	(21.9)
2G	5.3	(5.4)	18.8	(13.9)	**2G**$^-$	8.5	(8.8)	17.9	(13.1)
2H	6.3	(5.6)	17.7	(13.6)	**2H**$^-$	0.3	(0.3)	26.0	(21.7)
2I	6.6	(6.3)	17.4	(12.9)	**2I**$^-$	3.8	(3.5)	22.5	(18.4)
2J	7.1	(6.4)	16.9	(12.8)	**2J**$^-$	1.2	(1.5)	25.1	(20.4)
2K	7.4	(7.1)	16.6	(12.2)	**2K**$^-$	1.1	(1.0)	25.2	(21.0)
2L	8.7	(8.1)	15.4	(11.1)	**2L**$^-$	5.3	(5.4)	21.0	(16.5)
2M	12.0	(10.7)	12.0	(8.5)	**2M**$^-$	1.7	(1.6)	24.7	(20.3)
2N	11.9	(10.7)	12.1	(8.5)	**2N**$^-$ [d]	2.1	(2.2)	24.2	(19.8)

[a] Relative to the lowest-lying structure among anionic or neutral structures with a given hydration number. [b] Enthalpy (0 K) of the reaction: $\mathrm{AU{\cdot}(H_2O)_n \rightarrow AU + \mathit{n}H_2O}$. [c] Enthalpy (0 K) of the reaction: $\mathrm{[AU{\cdot}(H_2O)_n]^- \rightarrow AU^- + \mathit{n}H_2O}$. [d] Structure **2N**$^-$ is the same as **2B**$^-$.

Results and Discussion

Five structures and fourteen structures have been found for the neutral mono- and dihydrates, respectively, and their fully optimized geometries are included as Supporting Information, along with those for the respective anions. The relative energies and hydration energies for the neutral hydrates of the AU base pair and their respective anions are reported in Table 1. For convenience, the neutral hydrates are denoted with a number followed by a letter. The number indicates the number of water molecules for a given structure, and the letter represents its relative energy among the structures with the same hydration number, based on their zero-point vibrational energy (ZPVE)-corrected energies. For example, **2C** means the third energetically most favorable structure of the neutral AU dihydrate. The corresponding anion for a given neutral hydrate is designated by a negative-sign superscript (e.g., **2C**$^-$).

A. Unhydrated AU Base Pair and its Anion. The optimized structures of the unhydrated neutral AU base pair and its

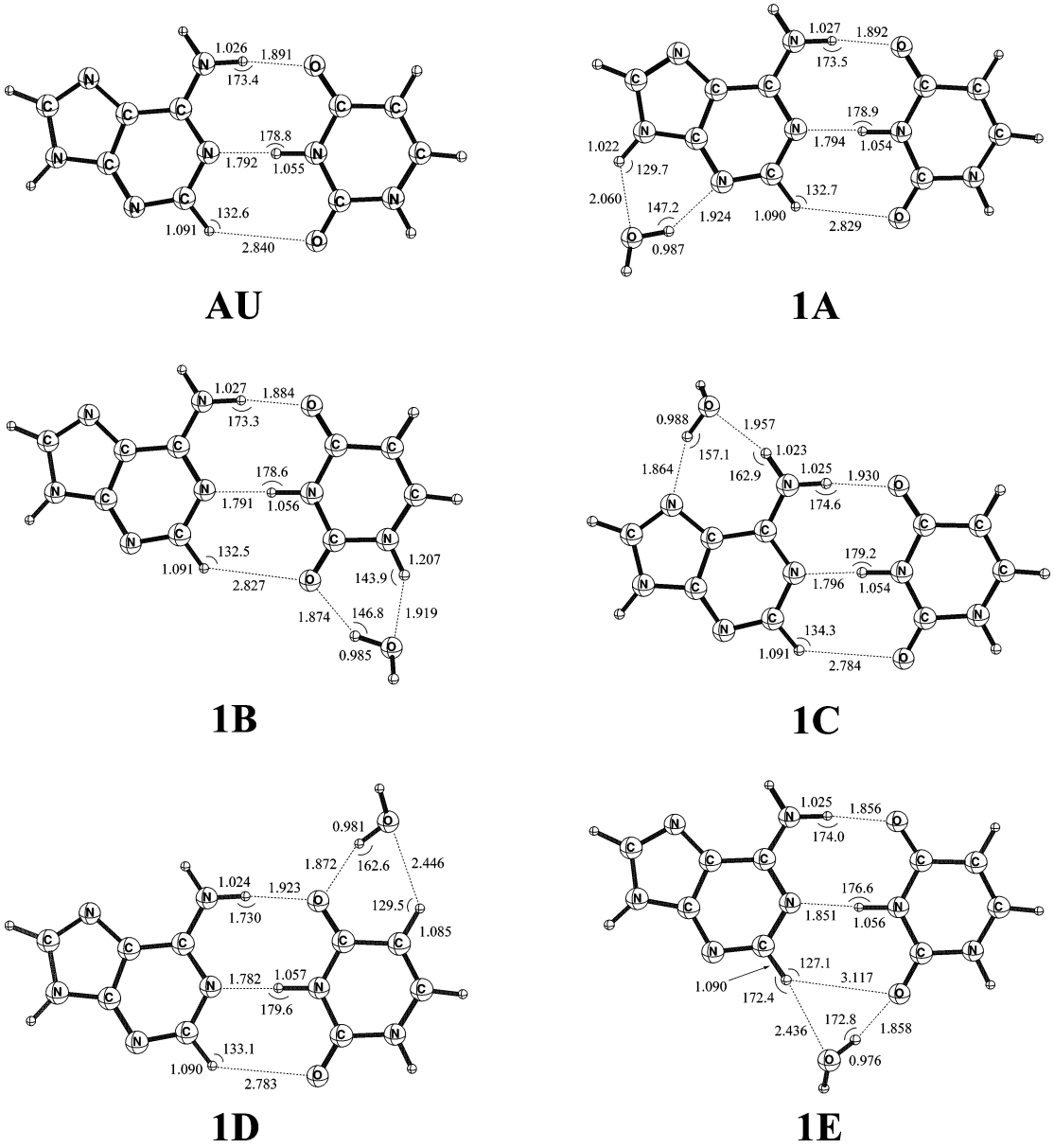

Figure 2. Molecular structures for the AU base pair and its monohydrates, optimized at the B3LYP/DZP++ level of theory.

monohydrates are shown in Figure 2, and the geometries of their respective anions are displayed in Figure 3. For the unhydrated neutral AU pair, the predicted $N_6-H_{6a}\cdots O_4$ and $N_1\cdots H-N_3$ hydrogen bond lengths were 1.891 and 1.792 Å, respectively. The $C_2-H\cdots O_2$ contact was predicted to be 2.840 Å. For the radical anion of the unhydrated AU pair, the interatomic $N_6-H_{6a}\cdots O_4$, $N_1\cdots H-N_3$, and $C_2-H\cdots O_2$ distances were 1.566, 2.072, and 3.487 Å, respectively.

Because the electron affinity of uracil is larger than that of adenine,[60] an additional electron in the anionic AU base pair is localized on the uracil moiety as implied in Figure 4, which shows the spin density plot of the radical anion of the AU pair. This negative charge density localized on the uracil moiety can be transferred to the adenine moiety through the $N_6-H_{6a}\cdot\cdot O_4$ hydrogen bond, where the uracil O_4 atom behaves as a hydrogen bond acceptor and the adenine H_{6a} atom acts as a hydrogen bond donor. Due to this effect, the $N_6-H_{6a}\cdots O_4$ hydrogen bond in the radical anion of the AU pair becomes much stronger than that for the neutral AU pair. Electron attachment to the neutral AU pair results in a decrease in the $N_6-H_{6a}\cdots O_4$ hydrogen bond length by 0.325 Å (from 1.891 to 1.566 Å). On the contrary, the $N_1\cdots H-N_3$ hydrogen bond is predicted to be weakened, because electron density would be transferred from the adenine to uracil moiety when the N_1-H hydrogen of uracil behaves as a hydrogen bond donor. Upon electron attachment to the AU base pair, the $N_1\cdots H-N_3$ hydrogen bond is predicted to increase by 0.280 Å (from 1.792 to 2.072 Å).

B. Monohydrates. For the monohydrate of the neutral AU base pair, five distinct structures have been found (Figure 2). In the lowest-energy structure, **1A**, a water molecule binds to the adenine moiety of the AU pair through a $N_9-H\cdots O_w-H_w\cdots N_3$ cyclic hydrogen bond. The second-lowest monohydrate, **1B**, in which a water molecule is associated with the uracil moiety by forming a $N_1-H\cdots O_w-H_w\cdots O_2$ cyclic hydrogen bond, was predicted to lie 0.3 kcal mol^{-1} above **1A**. Note that the hydrogen atoms at the adenine N_9 and the uracil N_1 positions are replaced with the pentose sugar units in DNA. Thus the hydrated species **1A** and **1B** may not be found routinely in actual DNA.

Compared to the unhydrated AU pair, the binding of the water molecules in **1A** and **1B** does not cause a significant change in the $N_6-H_{6a}\cdots O_4$ and $N_1\cdots H-N_3$ intermolecular hydrogen bond

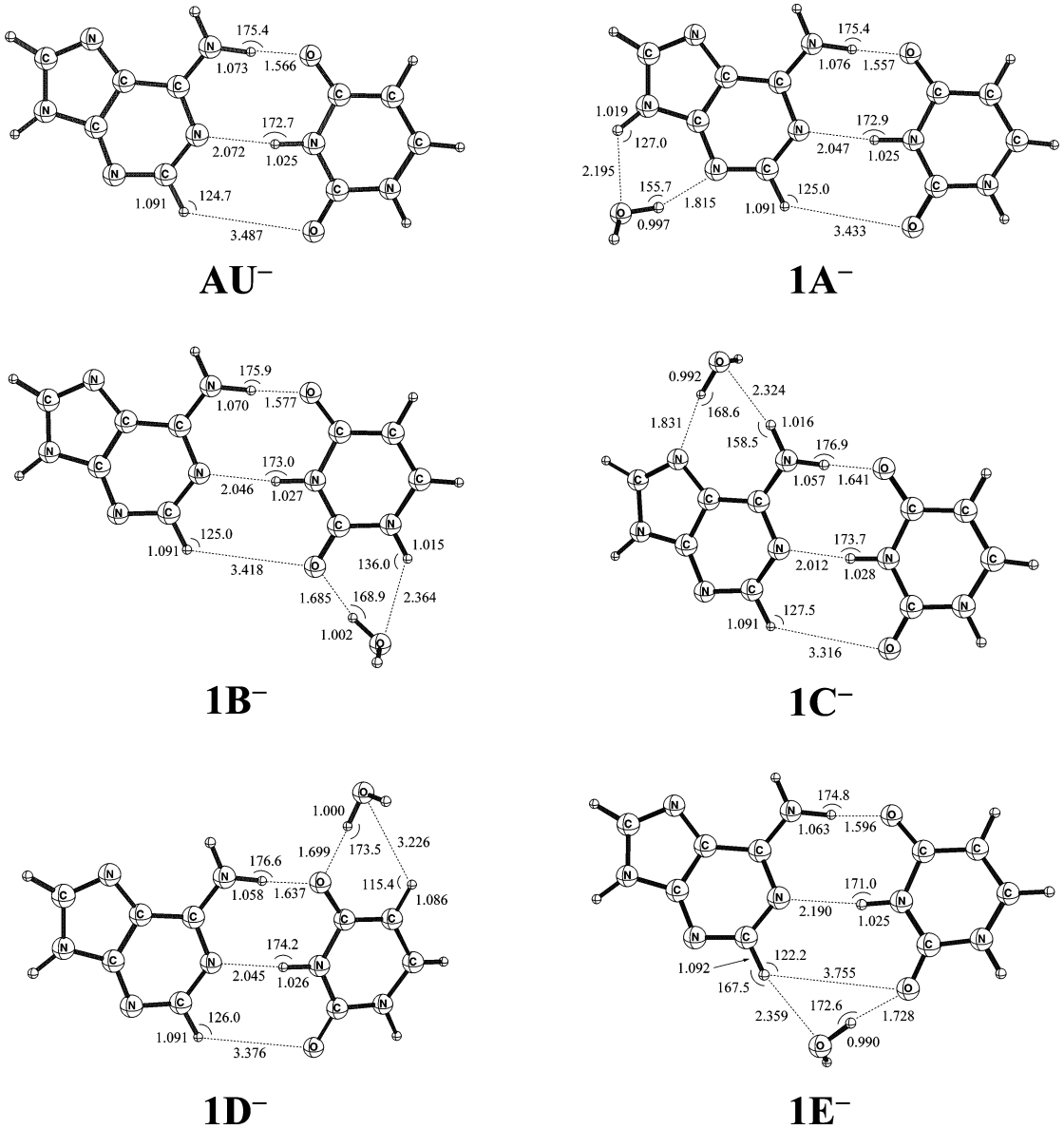

Figure 3. Molecular structures for the anion of the AU base pair and its monohydrates, optimized at the B3LYP/DZP++ level of theory.

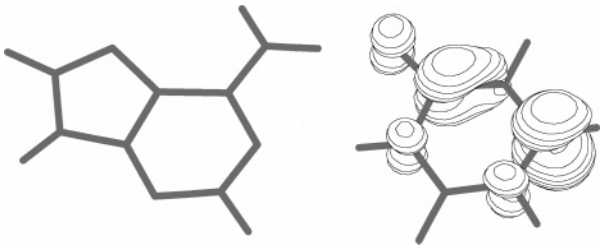

Figure 4. Spin density plot for the anion of the unhydrated AU base pair.

between the adenine and uracil bases. The largest difference was predicted to be 0.007 Å for the $N_6-H_{6a}\cdots O_4$ hydrogen bond in **1B**. The change in the weak $C_2-H\cdots O_2$ contact upon hydration to form **1A** and **1B** was also small (~0.01 Å). In structure **1C**, which is higher in energy than **1A** by 1.4 kcal mol^{-1}, a water molecule binds to the adenine moiety via the N_6-H_{6b} and N_7 atoms. Upon hydration to form **1C**, the $N_6-H_{6a}\cdots O_4$ hydrogen bond elongates by 0.039 Å, and the $N_1\cdots H-N_3$ hydrogen bond becomes longer by 0.004 Å.

All three lowest-energy structures of the neutral monohydrate of the AU base pair exhibit an $N-H\cdots O_w-H_w\cdots N$ or an $N-H\cdots O_w-H_w\cdots O$ cyclic hydrogen bond. On the other hand, the other two monohydrates, **1D** and **1E**, involve $C-H\cdots O$ contacts between the water molecule and one of the bases. Because these $C-H\cdots O$ contacts are weaker than a $N-H\cdots O$ or $O-H\cdots O$ hydrogen bond, the energies of structures **1D** and **1E** were predicted to be higher than that of the global minimum, **1A**, by 3.8 and 5.3 kcal mol^{-1}, respectively. While the hydration energies of the three lowest-energy structures, **1A**, **1B**, and **1C**, are predicted to range from 7.5 to 8.9 kcal mol^{-1}, those of **1D** and **1E** are smaller than the dimerization energy of water (D_e = 5.6 kcal mol^{-1} at the B3LYP/DZP++ level of theory).

For all five anionic monohydrates of the AU pair, the excess electron is found to be localized on the uracil moiety, similar to the case of the unhydrated AU radical anion. Thus, the geometries of the anionic AU monohydrates are also characterized by a decrease of the $N_6-H_{6a}\cdots O_4$ hydrogen bond distance and an increase of the $N_1\cdots H-N_3$ internuclear separation, compared to the corresponding neutrals. For the anionic monohydrates, the water molecule also plays an important role in stabilizing and/or destabilizing the anion of the AU pair. If a hydrogen atom of the water molecule forms a hydrogen bond with the anionic AU pair (like the $O_w-H_w\cdots N$

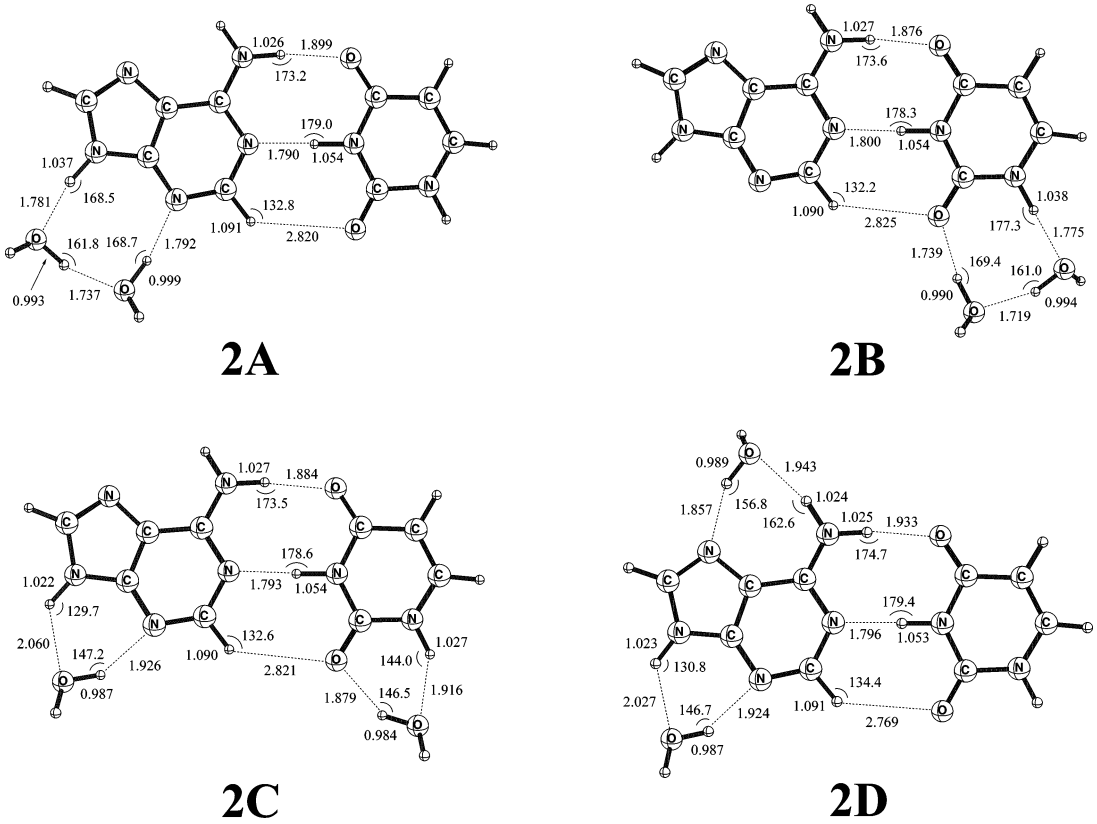

Figure 5. The four lowest-energy structures for the dihydrate of the neutral AU base pair.

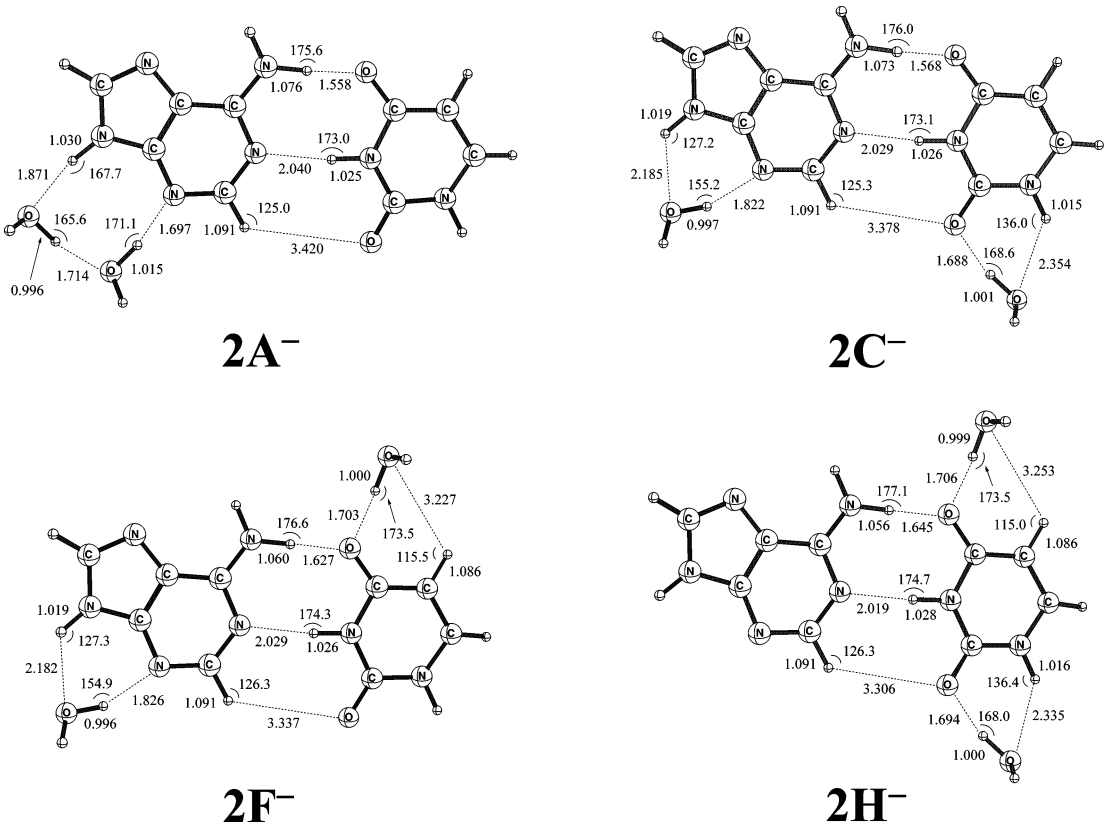

Figure 6. The four lowest-energy structures for the dihydrate of the AU base pair anion.

or the $O_w-H_w\cdots O$ hydrogen bond), the water molecule can stabilize the system by withdrawing electron density. On the other hand, when the water oxygen atom participates in hydrogen bonding with the anionic base pair (such as $N-H\cdots O_w$), it will destabilize the system by donating more electron density to the base pair. Note that anion **1D**$^-$ has a $C_5-H\cdots O_w$ contact (1.699 Å) between the water and the uracil moiety. Because the C−H hydrogen is not a good hydrogen bond donor, the unfavorable electron density transfer from water to uracil cannot be significant, while the water molecule can still stabilize the

system by pulling the negative charge density localized on the uracil through the $O_w-H_w\cdots O_4$ hydrogen bond. For this reason, anion **1D**$^-$ has the lowest energy among the five anionic monohydrates while the corresponding neutral, **1D**, is higher in energy than the three lowest-energy structures, **1A**, **1B**, and **1C**. The latter three structures have $N-H\cdots O_w$ hydrogen bonds (instead of $C-H\cdots O_w$ contacts), and upon electron attachment, these hydrogen bonds may force the unfavorable electron density donation from the water to the AU base pair, leading to further localization of negative charge on the uracil moiety. The relative energy of anion **1E**$^-$, which also has a $C-H\cdots O_w$ contact (2.359 Å), may also be understood in this context. That is, while structure **1E** has a higher energy than **1A** by 5.3 kcal mol^{-1}, the corresponding anion, **1E**$^-$, lies only 1.5 kcal mol^{-1} above **1A**$^-$.

C. Dihydrates. Fourteen structures have been found for the dihydrate of the neutral AU base pair and the four lowest-energy structures are displayed in Figure 5. For the lowest-energy structure, **2A**, both water molecules participate in the $N_9-H\cdots O_w$-$H_w\cdots O_w$-$H_w\cdots N_3$ cyclic hydrogen bond. Compared to monohydrate **1A**, this hydrogen-bonding motif (**2A**) involving two water molecules allows the nearly linear arrangement of the hydrogen bond donors and acceptors. For example, the $N_9-H\cdots O_w$ and O_w-$H_w\cdots N_3$ bond angles for **2A** are predicted to be 168.5° and 168.7°, respectively, while the corresponding values for **1A** are 129.7° and 147.2°, respectively. Thus, the resulting hydrogen bonds in **2A** are much stronger than those in **1A**, as implied in the shorter $N_9-H\cdots O_w$ and O_w-$H_w\cdots N_3$ hydrogen bond distances in **2A**. Similarly, the second lowest-lying structure, **2B**, which lies only 0.6 kcal mol^{-1} above **2A**, has a related $N_1-H\cdots O_w$-$H_w\cdots O_w$-$H_w\cdots O_2$ cyclic hydrogen bond.

In structure **2C**, which is higher in energy than **2A** by 1.9 kcal mol^{-1}, a water molecule binds to the adenine moiety via the N_9-H and N_3 atoms and the other water to the uracil unit via the N_1-H and O_2 atoms. This structure can be considered as a conjunction of the two lowest-lying structures, **1A** and **1B**. The hydrogen bond lengths for **2C** are very similar to those of **1A** and **1B**. The hydration energy for **2C** (17.4 kcal mol^{-1}) is almost the same as the sum of those for **1A** and **1B** (8.9 and 8.5 kcal mol^{-1}, respectively). Again the three lowest-lying anionic dihydrates (**2A**, **2B**, and **2C**) may not be relevant in DNA, where the adenine N9 and the uracil N1 atoms are connected to the pentose sugar units.

Figure 6 displays the four lowest-energy structures for the anionic dihydrate of the AU base pair. Similar to the case of the monohydrates, the energetic ordering for the anionic dihydrates is different from that for the neutral dihydrates. For the two lowest-energy structures, **2F**$^-$ and **2H**$^-$, a water molecule has a $C_5-H\cdots O_w$ contact, which does not allow negative charge density transfer from the water to the uracil moiety. The anionic dihydrates **2F**$^-$ and **2H**$^-$ have relative energies similar to that of **2A**$^-$, while the corresponding neutrals, **2F** and **2H**, are higher in energy than **2A**, by more than 5 kcal mol^{-1}. Two other interesting structures are the highest-energy neutral dihydrate found here, **2N**, and its anion. As shown in Figure 7, **2N** has a $C-H\cdots O_w$ contact (2.413 Å) between the adenine C_2-H and the oxygen atom of a water molecule. Electron attachment to **2N** results in the loss of the $C-H\cdots O$ contact; the anion geometry optimization using **2N** as an initial structure collapses to **2B**$^-$ structure, which is the corresponding anion of **2B**.

D. Electron Affinities. Table 2 lists VDEs and AEAs for the adenine−uracil base pair and its mono- and dihydrates, as well as the isolated adenine and uracil bases. The AEA_{abs} values for the AU base pair and its hydrates are summarized in Table

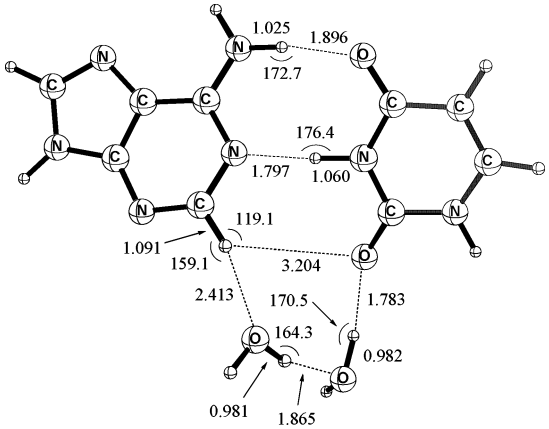

2N

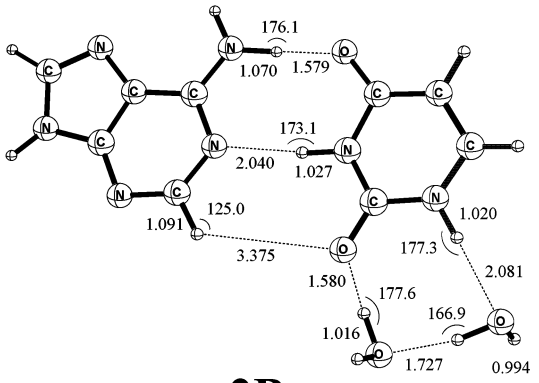

2B$^-$

Figure 7. The highest-energy (among structures considered) neutral dihydrate, **2N**, of the AU base pair and the corresponding anion **2B**$^-$. Electron attachment to **2N** causes the loss of the $C_2-H\cdots O_2$ contact, leading to migration of a water molecule. The resulting anion is identical to **2B**$^-$, which is the corresponding anion of **2B**.

TABLE 2: Vertical Detachment Energies (VDEs) and Local Adiabatic Electron Affinities (AEA_{local}'s) in eV for the Adenine-Uracil Base Pair and Its Mono- and Dihydrates (ZPVE-Corrected Values in Parentheses)

structure	VDE	AEA_{local}	
adenine	-0.30	-0.39	(−0.30)
uracil	0.76	0.12	(0.24)
AU	0.96	0.25	(0.40)
1A/1A$^-$	1.02	0.33	(0.49)
1B/1B$^-$	1.11	0.34	(0.49)
1C/1C$^-$	0.69	0.23	(0.42)
1D/1D$^-$	1.29	0.54	(0.68)
1E/1E$^-$	1.28	0.53	(0.65)
2A/2A$^-$	1.04	0.35	(0.51)
2B/2B$^-$	1.00	0.29	(0.45)
2C/2C$^-$	1.17	0.42	(0.57)
2D/2D$^-$	0.68	0.30	(0.50)
2E/2E$^-$	0.89	0.31	(0.50)
2F/2F$^-$	1.36	0.61	(0.75)
2G/2G$^-$	0.46	0.22	(0.37)
2H/2H$^-$	1.42	0.62	(0.75)
2I/2I$^-$	1.15	0.48	(0.64)
2J/2J$^-$	1.36	0.61	(0.73)
2K/2K$^-$	1.51	0.63	(0.79)
2L/2L$^-$	1.27	0.50	(0.64)
2M/2M$^-$	1.59	0.80	(0.92)
2N/2N$^-$ [a]	1.00	0.78	(0.89)

[a] Structure **2N**$^-$ is the same as **2B**$^-$.

TABLE 3: Absolute Adiabatic Electron Affinities (AEA_{abs}) in eV of the AU Base Pair and Its Mono- and Dihydrates (ZPVE-Corrected Values in Parentheses)

hydration number	structure	AEA_{abs}	
0		0.25	(0.40)
1	**1A/1D**$^-$	0.36	(0.51)
2	**2A/2F**$^-$	0.36	(0.52)

3. The ZPVE-corrected AEAs for adenine and uracil were predicted at the B3LYP/DZP++ level of theory to be −0.30 and 0.24 eV, respectively, implying that while the adenine anion is not valence bound, the uracil anion is weakly bound. Due to uracil having the greater AEA than adenine, the additional electron in the anion of the AU base pair was found to be largely localized on the uracil moiety, while the adenine unit may be considered to stabilize the anionic uracil through hydrogen bonding. From Figure 8, which shows pathways of the hydrate formation of the neutral and anionic AU base pairs from the isolated adenine and uracil, the following equation may be derived:

$$\mathrm{AEA(AU)} - \mathrm{AEA(U)} = E_{\mathrm{dis}}(\mathrm{AU}^-) - E_{\mathrm{dis}}(\mathrm{AU})$$

That is, the difference between the AEA of the isolated uracil and that of the AU base pair [AEA(AU) − AEA(U)] is equivalent to the difference in hydrogen-bonding strength (base pairing energy) between the AU base pair and its anion [$E_{\mathrm{dis}}(\mathrm{AU}^-) - E_{\mathrm{dis}}(\mathrm{AU})$]. At the B3LYP/DZP++ level of theory, the ZPVE-corrected dissociation energy of AU was computed to be 12.7 kcal mol^{-1} for the neutral AU pair and the 16.4 kcal mol^{-1} for its anion, and the difference of 3.7 kcal mol^{-1} (0.16 eV) results in the greater electron affinity of the AU base pair, compared to the isolated uracil. Similarly, the VDE for the AU is predicted to be larger by 0.20 eV than that of the isolated uracil.

Figure 8 also allows us to derive the following equation associated with the effect of hydration on the AEA of the AU base pair:

$$\mathrm{AEA[AU{\cdot}(H_2O)}_n\mathrm{]} - \mathrm{AEA(AU)} = E_{\mathrm{hyd}}(\mathrm{AU}^-) - E_{\mathrm{hyd}}(\mathrm{AU})$$

This equation implies that the change in hydration energy upon electron attachment is the sole source of the increased AEA of the AU hydrates. For example, as shown in Table 1, E_{hyd} of the lowest-lying anionic monohydrate, **1D**$^-$, is larger by 6.3 kcal mol^{-1} (=0.28 eV) than that of the corresponding neutral, **1D**. This corresponds to an increase in the AEA of monohydrate **1D** (0.68 eV), compared to the unhydrate AU base pair (0.40 eV). As mentioned above, upon electron attachment to the hydrates of the AU base pair, a water molecule can stabilize the system by withdrawing negative charge density localized on the uracil base through the hydrogen bond, where the water molecule acts as a hydrogen bond donor (e.g., the $O_w-H_w\cdots N$ and $O_w-H_w\cdots O$ hydrogen bonds). This effect is so strong that E_{hyd} values of the anionic hydrates are almost always larger than those of the corresponding neutrals, as reported in Table 1. As a result, microhydration of the AU base pair increases its AEA in general. For the dihydrate, the AEA increases up to 0.92 eV (for structure **2M**$^-$), and the AEA value for the lowest-lying anionic dihydrate, **2F**$^-$, is predicted to be 0.75 eV.

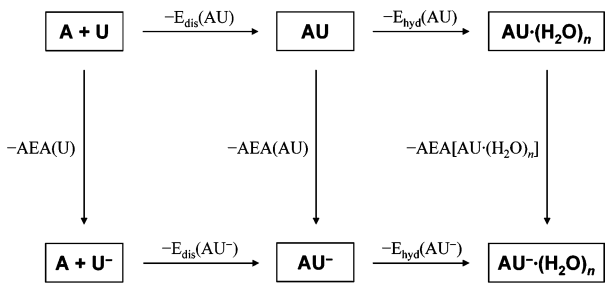

Figure 8. Schematic diagram showing pathways of the hydrate formation of the neutral and anionic AU base pair from the isolated adenine and uracil.

Conclusions

Microhydration effects upon the AU base pair and its radical anion have been studied by explicitly considering various structures for their mono- and dihydrates. In the present study five structures and fourteen structures have been found for the neutral mono- and dihydrates, respectively. For the three lowest-lying structures (**1A**, **1B**, and **1C**) of the neutral monohydrate, the water molecule forms a $N-H\cdots O_w-H_w\cdots N$ or a $N-H\cdots O_w-H_w\cdots O$ cyclic hydrogen bond, and their hydration energies are greater than 7.5 kcal mol^{-1}, assuring formation of these hydrates in aqueous solution. On the contrary, the other two neutral monohydrates (**1D** and **1E**) each have a weak $C-H\cdots O$ contact (instead of a strong $N-H\cdots O$ hydrogen bond) and cannot form the strong cyclic hydrogen bond found in the energetically more favorable structures. The small hydration energies of **1D** and **1E** imply that association of water with the AU base pair to form **1D** and **1E** competes with the dimerization between water molecules.

Similarly, each of the low-energy structures (**2A**, **2B**, and **2C**) for the neutral dihydrate has a cyclic hydrogen bond between the water molecules and the AU base pair, while the high-lying structures (**2D** and **2E**) have a $C-H\cdots O$ contact. The lowest-energy structures **2A** and **2B** of the neutral dihydrate are characterized by a cyclic hydrogen bond involving two water molecules, which can result in stronger hydrogen bonding due to the linear arrangement of hydrogen bond donors and acceptors.

Due to uracil having a greater electron attracting capability than adenine, an excess electron attached to the AU base pair occupies the π^* orbital of the uracil moiety. The negative charge density developed on the uracil moiety may be transferred to either the adenine moiety or hydrating water molecules when the uracil moiety participates in hydrogen bonding as a hydrogen bond acceptor (e.g., the $N_6-H_{6a}\cdots O_4$ hydrogen bond in the AU pair and the $O_w-H_w\cdots N$ and $O_w-H_w\cdots O$ hydrogen bonds between the AU pair and the water molecules). In addition, anionic structures which have $C-H\cdots O$ contacts are energetically more favorable than those with $N-H\cdots O$ hydrogen bonds, because the $C-H\cdots O$ contacts do not allow the unfavorable electron density donation from the water to the uracil moiety. For this reason, the energetic ordering of the anionic hydrates is predicted to be quite different from that of the corresponding neutral hydrates.

The electron affinity of the AU base pair was found to significantly increase upon hydration. While the VDE and AEA of the unhydrated AU base pair were 0.96 and 0.40 eV, respectively, the corresponding values for the lowest-energy anionic dihydrate were predicted to be 1.36 and 0.75 eV, respectively. The latter value (0.75 eV) is the energy difference between the global anion minimum **2F**$^-$ and the neutral local structure **2F** analogous to **2F**$^-$. The AEA_{abs} values were predicted to be 0.51 and 0.52 eV for the mono- and dihydrates, respectively. For all anionic structures considered in the present study, an excess electron was found to occupy the π^* orbital of the uracil moiety. The RET spectroscopic study of Periquet

et al.[66] showed that at least two hydrating water molecules are necessary to form a stable valence-bound anion of the isolated adenine. On the other hand, the AEA of uracil is positive even in the absence of hydrating water molecules. Therefore, the uracil moiety in the AU base pair and its hydrates is far more favorable for electron attachment.

Acknowledgment. This work was supported by the U.S. National Science Foundation under Grant No. CHE-0451445.

Supporting Information Available: Geometries for the neutral and anionic AU base pairs and their mono- and di-hydrates, optimized at the B3LYP/DZP++ level of theory. This material is available free of charge via the Internet at http://pubs.acs.org.

References and Notes

(1) Ries, G.; Heller, W.; Puchta, H.; Sandermann, H.; Seidlitz, H. K.; Hohn, B. *Nature* **2000**, *406*, 98.
(2) Kovalchuk, O.; Dubrova, Y. E.; Arkhipov, A.; Hohn, B.; Kovalchuk, I. *Nature* **2000**, *407*, 583.
(3) Grosovsky, A. J. *Proc. Natl. Acad. Sci. U.S.A.* **1999**, *96*, 5346.
(4) Wu, L. J.; Randers-Pehrson, G.; Xu, A.; Waldren, C. A.; Geard, C. R.; Yu, Z.; Hei, T. K. *Proc. Natl. Acad. Sci. U.S.A.* **1999**, *96*, 4959.
(5) Morgan, W. F.; Sowa, M. B. *Proc. Natl. Acad. Sci. U.S.A.* **2005**, *102*, 14127.
(6) Belyakov, O. V.; Mitchell, S. A.; Parikh, D.; Randers-Pehrson, G.; Marino, S. A.; Amundson, S. A.; Geard, C. R.; Brenner, D. J. *Proc. Natl. Acad. Sci. U.S.A.* **2005**, *102*, 14203.
(7) Sutherland, B. M.; Bennett, P. V.; Sidorkina, O.; Laval, J. *Proc. Natl. Acad. Sci. U.S.A.* **2000**, *97*, 103.
(8) Tusher, V. G.; Tibshirani, R.; Chu, G. *Proc. Natl. Acad. Sci. U.S.A.* **2001**, *98*, 5116.
(9) Cathcart, R.; Schwiers, E.; Saul, R. L.; Ames, B. N. *Proc. Natl. Acad. Sci. U.S.A.* **1984**, *81*, 5633.
(10) Haranczyk, M.; Rak, J.; Gutowski, M.; Radisic, D.; Stokes, S. T.; Bowen, K. H. *J. Phys. Chem. B* **2005**, *109*, 13383.
(11) Haranczyk, M.; Dabkowska, I.; Rak, J.; Gutowski, M.; Nilles, J. M.; Stokes, S.; Radisic, D.; Bowen, K. H. *J. Phys. Chem. B* **2004**, *108*, 6919.
(12) Kroeger, K. M.; Jiang, Y. L.; Kow, Y. W.; Goodman, M. F.; Greenberg, M. M. *Biochemistry* **2004**, *43*, 6723.
(13) Kroeger, K. M.; Kim, J.; Goodman, M. F.; Greenberg, M. M. *Biochemistry* **2004**, *43*, 13621.
(14) Kim, J.; Weledji, Y. N.; Greenberg, M. M. *J. Org. Chem.* **2004**, *69*, 6100.
(15) Kodama, T.; Greenberg, M. M. *J. Org. Chem.* **2005**, *70*, 9916.
(16) Hong, I. S.; Greenberg, M. M. *J. Am. Chem. Soc.* **2005**, *127*, 3692.
(17) Hong, I. S.; Greenberg, M. M. *J. Am. Chem. Soc.* **2005**, *127*, 10510.
(18) Hong, I. S.; Ding, H.; Greenberg, M. M. *J. Am. Chem. Soc.* **2006**, *128*, 485.
(19) Hong, I. S.; Ding, H.; Greenberg, M. M. *J. Am. Chem. Soc.* **2006**, *128*, 2230.
(20) Boudaiffa, B.; Cloutier, P.; Hunting, D.; Huels, M. A.; Sanche, L. *Science* **2000**, *287*, 1658.
(21) Michael, B. D.; O'Neill, P. *Science* **2000**, *287*, 1603.
(22) Datta, K.; Neumann, R. D.; Winters, T. A. *Proc. Natl. Acad. Sci. U.S.A.* **2005**, *102*, 10569.
(23) Cauet, E.; Dehareng, D.; Lievin, J. *J. Phys. Chem. A* **2006**, *110*, 9200.
(24) Sun, L.; Bu, Y. *J. Phys. Chem. B* **2005**, *109*, 593.
(25) Purkayastha, S.; Bernhard, W. A. *J. Phys. Chem. B* **2004**, *108*, 18377.
(26) Choi, K.-W.; Lee, J.-H.; Kim, S. K. *J. Am. Chem. Soc.* **2005**, *127*, 15674.
(27) Crespo-Hernandez, C. E.; Arce, R.; Ishikawa, Y.; Gorb, L.; Leszczynski, J.; Close, D. M. *J. Phys. Chem. A* **2004**, *108*, 6373.
(28) Li, X.; Cai, Z.; Sevilla, M. D. *J. Phys. Chem. A* **2002**, *106*, 9345.
(29) Bertran, J.; Oliva, A.; Rodriguez-Santiago, L.; Sodupe, M. *J. Am. Chem. Soc.* **1998**, *120*, 8159.
(30) Kim, S. K.; Lee, W.; Herschbach, D. R. *J. Phys. Chem.* **1996**, *100*, 7933.
(31) Kanvah, S.; Schuster, G. B. *J. Am. Chem. Soc.* **2002**, *124*, 11286.
(32) Ghosh, A. K.; Schuster, G. B. *J. Am. Chem. Soc.* **2006**, *128*, 4172.
(33) Sugiyama, H.; Saito, I. *J. Am. Chem. Soc.* **1996**, *118*, 7063.
(34) Gervasio, F. L.; Laio, A.; Iannuzzi, M.; Parrinello, M. *Chem. Eur. J.* **2004**, *10*, 4846.
(35) Ratner, M. *Nature* **1999**, *397*, 480.
(36) Meggers, E.; Michel-Beyerle, M. E.; Giese, B. *J. Am. Chem. Soc.* **1998**, *120*, 12950.
(37) Pratviel, G.; Meunier, B. *Chem. Eur. J.* **2006**, *12*, 6018.
(38) Swiderek, P. *Angew. Chem., Int. Ed.* **2006**, *45*, 4056.
(39) Sanche, L. *Eur. Phys. J. D* **2005**, *35*, 367.
(40) Sanche, L. *Phys. Scr.* **2003**, *68*, C108.
(41) Li, X.; Sevilla, M. D.; Sanche, L. *J. Phys. Chem. B* **2004**, *108*, 19013.
(42) Ptasinska, S.; Denifl, S.; Scheier, P.; Illenberger, E.; Maerk, T. D. *Angew. Chem., Int. Ed.* **2005**, *44*, 6941.
(43) Ptasinska, S.; Denifl, S.; Gohlke, S.; Scheier, P.; Illenberger, E.; Maerk, T. D. *Angew. Chem., Int. Ed.* **2006**, *45*, 1893.
(44) Ptasinska, S.; Denifl, S.; Grill, V.; Maerk, T. D.; Scheier, P.; Gohlke, S.; Huels, M. A.; Illenberger, E. *Angew. Chem., Int. Ed.* **2005**, *44*, 1647.
(45) Cobut, V.; Frongillo, Y.; Patau, J. P.; Goulet, T.; Fraser, M. J.; Jay-Gerin, J. P. *Radiat. Phys. Chem.* **1998**, *51*, 229.
(46) Ray, S. G.; Daube, S. S.; Naaman, R. *Proc. Natl. Acad. Sci. U.S.A.* **2005**, *102*, 15.
(47) Simons, J. *Acc. Chem. Res.* **2006**, *39*, 772.
(48) Li, X.; Sevilla, M. D.; Sanche, L. *J. Am. Chem. Soc.* **2003**, *125*, 13668.
(49) Bao, X.; Wang, J.; Gu, J.; Leszczynski, J. *Proc. Natl. Acad. Sci. U.S.A.* **2006**, *103*, 5658.
(50) Gu, J.; Wang, J.; Leszczynski, J. *J. Am. Chem. Soc.* **2006**, *128*, 9322.
(51) Bald, I.; Kopyra, J.; Illenberger, E. *Angew. Chem., Int. Ed.* **2006**, *45*, 4851.
(52) Martin, F.; Burrow, P. D.; Cai, Z.; Cloutier, P.; Hunting, D.; Sanche, L. *Phys. Rev. Lett.* **2004**, *93*, 068101.
(53) Zheng, Y.; Cloutier, P.; Hunting, D. J.; Sanche, L.; Wagner, J. R. *J. Am. Chem. Soc.* **2005**, *127*, 16592.
(54) Oyler, N. A.; Adamowicz, L. *J. Phys. Chem.* **1993**, *97*, 11122.
(55) Oyler, N. A.; Adamowicz, L. *Chem. Phys. Lett.* **1994**, *219*, 223.
(56) Roehrig, G. H.; Oyler, N. A.; Adamowicz, L. *J. Phys. Chem.* **1995**, *99*, 14285.
(57) Desfrancois, C.; Abdoul-Carime, H.; Schermann, J. P. *J. Chem. Phys.* **1996**, *104*, 7792.
(58) Hendricks, J. H.; Lyapustina, S. A.; de Clercq, H. L.; Snodgrass, J. T.; Bowen, K. H. *J. Chem. Phys.* **1996**, *104*, 7788.
(59) Sevilla, M. D.; Besler, B.; Colson, A. O. *J. Phys. Chem.* **1994**, *98*, 2215.
(60) Wesolowski, S. S.; Leininger, M. L.; Pentchev, P. N.; Schaefer, H. F. *J. Am. Chem. Soc.* **2001**, *123*, 4023.
(61) Schiedt, J.; Weinkauf, R.; Neumark, D. M.; Schlag, E. W. *Chem. Phys.* **1998**, *239*, 511.
(62) Kim, S.; Schaefer, H. F. *J. Chem. Phys.* **2006**, *125*, 144305.
(63) Kim, S.; Wheeler, S. E.; Schaefer, H. F. *J. Chem. Phys.* **2006**, *124*, 204310.
(64) Kim, S.; Schaefer, H. F. *J. Chem. Phys.* **2007**, *126*, 064301.
(65) Kang, H.; Lee, K. T.; Kim, S. K. *Chem. Phys. Lett.* **2002**, *359*, 213.
(66) Periquet, V.; Moreau, A.; Carles, S.; Schermann, J. P.; Desfrancois, C. *J. Electron Spectrosc. Relat. Phenom.* **2000**, *106*, 141.
(67) Choi, M. Y.; Miller, R. E. *Phys. Chem. Chem. Phys.* **2005**, *7*, 3565.
(68) Hendricks, J. H.; Lyapustina, S. A.; de Clercq, H. L.; Bowen, K. H. *J. Chem. Phys.* **1998**, *108*, 8.
(69) Liu, D.; Wyttenbach, T.; Bowers, M. T. *J. Am. Chem. Soc.* **2006**, *128*, 15155.
(70) Morgado, C. A.; Pichugin, K. Y.; Adamowicz, L. *Phys. Chem. Chem. Phys.* **2004**, *6*, 2758.
(71) Hunter, K. C.; Rutledge, L. R.; Wetmore, S. D. *J. Phys. Chem. A* **2005**, *109*, 9554.
(72) Nugent, M. L.; Adamowicz, L. *Mol. Phys.* **2005**, *103*, 1467.
(73) Jalbout, A. F.; Adamowicz, L. *J. Phys. Chem. A* **2001**, *105*, 1033.
(74) Bao, X.; Sun, H.; Wong, N.-B.; Gu, J. *J. Phys. Chem. B* **2006**, *110*, 5865.
(75) Bao, X.; Liang, G.; Wong, N. B.; Gu, J. *J. Phys. Chem. A* **2007**, *111*, 666.
(76) Colson, A. O.; Besler, B.; Sevilla, M. D. *J. Phys. Chem.* **1993**, *97*, 13852.
(77) Kumar, A.; Mishra, P. C.; Suhai, S. *J. Phys. Chem. A* **2005**, *109*, 3971.
(78) Zendlova, L.; Hobza, P.; Kabelac, M. *ChemPhysChem* **2006**, *7*, 439.
(79) Shao, Y.; Molnar, L. F.; Jung, Y.; Kussmann, J.; Ochsenfeld, C.; Brown, S. T.; Gilbert, A. T. B.; Slipchenko, L. V.; Levchenko, S. V.; O'Neill, D. P.; DiStasio, R. A.; Lochan, R. C.; Wang, T.; Beran, G. J. O.; Besley, N. A.; Herbert, J. M.; Lin, C. Y.; Van Voorhis, T.; Chien, S. H.; Sodt, A.; Steele, R. P.; Rassolov, V. A.; Maslen, P. E.; Korambath, P. P.; Adamson, R. D.; Austin, B.; Baker, J.; Byrd, E. F. C.; Dachsel, H.; Doerksen, R. J.; Dreuw, A.; Dunietz, B. D.; Dutoi, A. D.; Furlani, T. R.; Gwaltney, S. R.; Heyden, A.; Hirata, S.; Hsu, C.-P.; Kedziora, G.; Khalliulin, R. Z.; Klunzinger, P.; Lee, A. M.; Lee, M. S.; Liang, W.; Lotan, I.; Nair,

N.; Peters, B.; Proynov, E. I.; Pieniazek, P. A.; Rhee, Y. M.; Ritchie, J.; Rosta, E.; Sherrill, C. D.; Simmonett, A. C.; Subotnik, J. E.; Woodcock, H. L.; Zhang, W.; Bell, A. T.; Chakraborty, A. K.; Chipman, D. M.; Keil, F. J.; Warshel, A.; Hehre, W. J.; Schaefer, H. F.; Kong, J.; Krylov, A. I.; Gill, P. M. W.; Head-Gordon, M. *Phys. Chem. Chem. Phys.* **2006**, *8*, 3172.

(80) Becke, A. D. *J. Chem. Phys.* **1993**, *98*, 5648.

(81) Lee, C.; Yang, W.; Parr, R. G. *Phys. Rev. B* **1988**, *37*, 785.

(82) Papas, B. N.; Schaefer, H. F. *J. Mol. Struct.* **2006**, *768*, 175.

(83) Huzinaga, S. *J. Chem. Phys.* **1965**, *42*, 1293.

(84) Dunning, T. H. *J. Chem. Phys.* **1970**, *53*, 2823.

(85) Lee, T. J.; Schaefer, H. F. *J. Chem. Phys.* **1985**, *83*, 1784.

(86) Rienstra-Kiracofe, J. C.; Tschumper, G. S.; Schaefer, H. F.; Nandi, S.; Ellison, G. B. *Chem. Rev.* **2002**, *102*, 231.